Predicting the arrival of high-speed solar wind streams at Earth using the STEREO Heliospheric Imagers

Article

Published Version

Predicting the arrival of high-speed solar wind streams at Earth using the STEREO Heliospheric Imagers

C. J. Davis,[1,2] J. A. Davies,[3] M. J. Owens,[1] and M. Lockwood[1]

Received 5 October 2011; revised 9 November 2011; accepted 11 December 2011; published 16 February 2012.

[1] High-speed solar wind streams modify the Earth's geomagnetic environment, perturbing the ionosphere, modulating the flux of cosmic rays into the Earth atmosphere, and triggering substorms. Such activity can affect modern technological systems. To investigate the potential for predicting the arrival of such streams at Earth, images taken by the Heliospheric Imager (HI) on the STEREO-A spacecraft have been used to identify the onsets of high-speed solar wind streams from observations of regions of increased plasma concentrations associated with corotating interaction regions, or CIRs. In order to confirm that these transients were indeed associated with CIRs and to study their average properties, arrival times predicted from the HI images were used in a superposed epoch analysis to confirm their identity in near-Earth solar wind data obtained by the Advanced Composition Explorer (ACE) spacecraft and to observe their influence on a number of salient geophysical parameters. The results are almost identical to those of a parallel superposed epoch analysis that used the onset times of the high-speed streams derived from east/west deflections in the ACE measurements of solar wind speed to predict the arrival of such streams at Earth, assuming they corotated with the Sun with a period of 27 days. Repeating the superposed epoch analysis using restricted data sets demonstrates that this technique can provide a timely prediction of the arrival of CIRs at least 1 day ahead of their arrival at Earth and that such advanced warning can be provided from a spacecraft placed 40° ahead of Earth in its orbit.

Citation: Davis, C. J., J. A. Davies, M. J. Owens, and M. Lockwood (2012), Predicting the arrival of high-speed solar wind streams at Earth using the STEREO Heliospheric Imagers, *Space Weather*, *10*, S02003, doi:10.1029/2011SW000737.

1. Introduction

[2] The arrival at Earth of high-speed solar wind streams has been shown to perturb the Earth's geomagnetic environment, modifying ionospheric parameters [*Denton et al.*, 2009] and triggering substorms. If the high-speed stream is long-lived these terrestrial effects will recur every 27 days, corresponding to the rotation rate of the Sun [*Hapgood*, 1993]. Such activity can affect modern technological systems by, for example, enhancing the radiation environment for polar orbiting spacecraft, generating geomagnetically induced currents (GICs) which affect ground-based power systems and disrupting HF communications used for trans-oceanic flights [*Hapgood*, 2011]. While the biggest potential for disruption to these systems comes from the arrival of energetic Earth-directed coronal mass ejections (CMEs), the recurrence and longevity of co-rotating streams demands that it is also desirable to forecast their arrival, particularly on the declining phase of the solar cycle when their influence is greatest [*Hapgood*, 1993]. *Borovsky and Denton* [2006] compared the influence of CMEs and CIRs on the Earth's space environment and concluded that while CMEs posed the greatest problem for ground-based power systems, CIRs posed more of a problem for space-based assets than CMEs due to higher levels of spacecraft charging.

[3] Until relatively recently, it has only been possible to predict the arrival of high-speed solar wind streams at Earth from observation of the solar disk, where the appearance of coronal holes at low solar latitudes indicated the potential for the resulting high-speed solar wind stream to reach Earth. A coronal hole is a region of the solar corona with relatively low intensity when viewed in extreme ultraviolet light. The solar magnetic fields in such regions extend out into the heliosphere and so provide little or no hindrance to the out-flowing solar wind plasma. The solar wind speed emanating from such regions is therefore usually relatively high while the plasma density

[1]Department of Meteorology, University of Reading, Reading, UK.
[2]Also at RAL Space, Rutherford Appleton Laboratory, Chilton, UK.
[3]RAL Space, Rutherford Appleton Laboratory, Chilton, UK.

is relatively low [e.g., *Wang and Sheeley*, 1990; *McComas et al.*, 2003]. The relationship between the coronal magnetic field and the solar wind speed has been investigated [*Arge and Pizzo*, 2000; *Riley et al.*, 2001] and has become one of the standard methods of predicting the arrival of high-speed solar wind streams at Earth.

[4] Predicting the arrival of high speed streams at Earth by observing coronal holes requires assumptions to be made about the evolution of such features as the Sun rotates and the influence of the ambient solar wind and interplanetary field as they propagate out into the heliosphere.

[5] The twin spacecraft of the NASA STEREO mission [*Kaiser et al.*, 2008] were designed to enable studies of the Sun and inner heliosphere in three dimensions. The spacecraft are in heliocentric orbits similar to that of the Earth, one drifting ahead of the Earth (STEREO-Ahead or STEREO-A) at a distance of approximately 0.96 astronomical units (AU) from the Sun while the other (STEREO-Behind or STEREO-B) lags behind the Earth at a distance of approximately 1.04 AU from the Sun. As a consequence of their orbits, the two observatories are moving away from the Earth at a rate that causes the Earth-Sun-spacecraft angle to increase by around 22.5° per year. Each spacecraft carries a suite of instrumentation to image the Sun and solar wind and make in situ measurements of the interplanetary medium.

[6] The SECCHI instrument package [*Howard et al.*, 2008] on each spacecraft includes a Heliospheric Imager [*Eyles et al.*, 2009]. This is an instrument containing two wide-field white-light cameras mounted on the side of the spacecraft to image any transients in the solar wind through Thomson scattering of sunlight by electrons in the solar wind plasma [*Billings*, 1966]. The sunward of the two HI cameras, HI1, has a 20° field of view with a bore-sight directed at 14° elongation from Sun center in the ecliptic plane. The outer camera, HI2, has a 70° field of view centered at 53.5° elongation. Between them, these two cameras can image the ecliptic from 4° to 74° from Sun-center. One of the primary goals of the STEREO mission was to track solar wind transients such as CMEs from the vantage point of two spacecraft, using the stereoscopic view to determine not only the speed but also the direction of such transients [e.g., *Liu et al.*, 2010].

[7] The HI cameras were the first to directly image the interface between slow and fast regions of solar wind by detecting localized plasma density enhancements entrained along the slow/fast stream interface. These enhancements, assumed to be propagating at the same speed as the stream interface, are seen to be moving radially outwards from the Sun and extend from 5°–10° in solar latitude [*Rouillard et al.*, 2010a]. While there is no information about their extent in solar longitude from the STEREO/HI images, such localized features form part of much larger, longitudinally extended, structures known as co-rotating interaction regions, or CIRs [*Sheeley et al.*, 2008; *Rouillard et al.*, 2008; *Tappin and Howard*, 2009]. Furthermore, it proved possible to accurately estimate the speed and direction of such features from their time-elongation profile out to large elongations by a single spacecraft. In order to do this, the transient is assumed to be traveling radially outwards from the Sun at a constant speed, v, along a trajectory for which the spacecraft-Sun-transient angle, φ, is also constant. A consideration of the geometry in the ecliptic plane reveals that the elongation angle of the transient from the Sun, α, is related to v and φ by the relation

$$\alpha(v,\varphi) = a\tan\left[\frac{D(t)\sin\varphi}{r(t) - D(t)\cos\varphi}\right] \quad (1)$$

where r(t) is the heliocentric radial distance of the spacecraft, D(t) is the distance of the transient from the Sun and t is the time of the observation. The velocity, v, can be determined from the rate f change of D(t). Due to the assumption that the transient has a fixed radial trajectory, this technique has become known as the "fixed phi" method. For such a relationship, a transient propagating at a constant radial velocity toward the observer (in this case, the STEREO spacecraft) will have an apparent acceleration while a transient propagating away from the observer will have an apparent deceleration. By assuming that a transient did not undergo significant changes in speed or direction as it propagated through the HI field of view it is possible to use the apparent acceleration of the transient to estimate its radial speed and direction relative to the observer by fitting the observed elongation-time profile for a range of values of v and φ and selecting the best fit. As the position of the spacecraft is known relative to the Earth, it is therefore possible to calculate the trajectory of the transient relative to Earth. Such an effect was initially considered for coronagraph data by *Sheeley et al.* [1999], was first used for CME tracking in data from the Solar Mass Ejection Imager [*Kahler and Webb*, 2007], and was subsequently applied to STEREO data by *Sheeley et al.* [2008] and *Rouillard et al.* [2008]. The authors corroborated their observations by comparison with in situ measurements of the speed, density, temperature, composition and magnetic field strength of the interplanetary medium made near the L1 Lagrangian point, using data from the Advanced Composition Explorer (ACE) located approximately 15,000,000 km upstream of the Earth [*Stone et al.*, 1998].

[8] The accuracy with which the speed and direction of a transient can be estimated is dependent on the quality and ambiguity of the fit between the data and the model values. *Williams et al.* [2009] used simulated data to show that a transient needed to be tracked over elongations of at least 30° for its speed and direction to be estimated with any accuracy. For individual CIR-associated transients tracked in the STEREO/HI data that were found to propagate directly toward Earth or one of the STEREO spacecraft, the accuracy of the predicted arrival times of the CIRs was within three hours of the measured arrival times [e.g., *Rouillard et al.*, 2009, 2010a, 2010b].

[9] The ability to estimate the speed and direction of solar wind transients from a single spacecraft has many advantages, particularly at phases of the mission where the separation between the two spacecraft is too large for stereoscopic views within the HI field of view. While the fixed-phi technique above is most applicable to spatially constrained transients such as plasma blobs that become entrained in CIRs, there continues to be subsequent refinement of the model to consider structures that have a much greater spatial extent such as CMEs [e.g., *Lugaz et al.*, 2009; *Möstl et al.*, 2009].

[10] The solar wind flows radially out from the Sun which rotates with a period of approximately 27 days. As a consequence, the solar wind is distorted into the Parker spiral form [*Parker*, 1963] which applies on average near the Earth [*Hapgood et al.*, 1991]. As the fast solar wind catches up with the slow solar wind ahead of it, plasma becomes concentrated along the slow/fast stream interface [e.g., *Pizzo*, 1991]. The HI cameras image localized enhancements in plasma density that become entrained along the stream interface, thereby enabling the position of the stream interface to be determined at those specific locations. Depending on the magnetic topology of the Sun, the region of high-speed solar wind could extend for many tens of degrees in the solar atmosphere resulting in a high-speed stream that could last for several days at Earth and recur for many months.

[11] The purpose of this study is to use observations of localized plasma enhancements to infer the location of CIRs in STEREO data and to determine whether it is possible to predict the arrival of fast solar wind streams at Earth by assuming that such features co-rotate with the Sun at a rate of 13.3° in solar longitude per day with respect to the Earth. The subsequent response of the Earth's magnetic field and upper atmosphere is then estimated by monitoring changes in various geomagnetic parameters. To do this, we carry out two separate superposed epoch studies using an analysis technique similar to that of *Denton et al.* [2009]. In one we use ACE in situ measurements to determine the arrival of high-speed streams at Earth and in the other we use the trajectories of CIR-associated transients determined from STEREO HI images to predict the arrival of high-speed solar wind streams ahead of their arrival at Earth.

2. Method

[12] The arrival of high-speed solar wind streams at ACE has been determined by looking for east/west deflections in the solar wind V_y component. This behavior is commonly used to identify such features [e.g., *McPherron et al.*, 2004; *Denton et al.*, 2009]. Around 146 features have been detected in the ACE data from the beginning of 2007 to 2010. The times of these signatures at ACE were used in a superposed epoch study to estimate the average behavior of solar wind and geophysical parameters.

[13] The signature of a CIR in ACE data consists of an increase in solar wind bulk flow speed that is accompanied by a density and magnetic field enhancement at the leading edge of the fast stream. In addition to investigating the average behavior of these solar wind parameters to the arrival of a high speed stream, the southward component of the interplanetary magnetic field (IMF) was also investigated since it is the size and duration of southward IMF that has a dominant effect on the efficiency with which the solar wind couples with the geomagnetic field. The influence of fast solar wind streams at Earth was also investigated by considering the response of several important geophysical data sets.

[14] The Ap index is a measure of the general level of disturbance in the Earth's magnetic field due to currents flowing in the Earth's ionosphere and magnetosphere. The index is defined over a period of one day from a set of standard stations around the world. As a result, the Ap index reflects the variability in the Earth's magnetic field either in direct response to changes in solar wind or to any subsequent geomagnetic storms.

[15] The Dst (disturbance storm time) index is a measure of equatorial geomagnetic disturbance derived from hourly measurements of the horizontal magnetic field component at low-latitudes. It is sensitive to the westward ring current flowing at high altitudes. When this current is enhanced it suppresses the horizontal component of the Earth's equatorial magnetic field.

[16] Cosmic rays entering the Earth's atmosphere are monitored on the ground by detecting the neutrons produced as the cosmic rays interact with the Earth's atmosphere. Such counts need to be corrected for atmospheric pressure and the energy threshold of a given station is a function of its geomagnetic latitude since cosmic rays are deflected by the Earth's magnetic field. Any enhancement and structure in the interplanetary field associated with structures in the solar wind will reduce the number of cosmic rays reaching Earth. We here employ data from the neutron monitoring station at Oulu, Finland, which extends back to 1964 and is one of many such stations which form a world-wide network.

[17] The Earth's ionosphere is a weak plasma predominantly generated by photo-ionisation of the Earth's upper atmosphere. It is traditionally probed by transmitting short-wave radio pulses which are reflected where the radio frequency matches the plasma frequency. The peak frequency reflected by each layer, fp, can be used to estimate the peak electron concentration of that layer, N, through the relationship $fp = 9\sqrt{N}$. The ionospheric F2-region lies at an altitude of around 250–400 km and is significantly influenced by geomagnetic activity. The peak frequency reflected by this layer is known as foF2. We here employ data from the ionospheric monitoring station at Chilton which continues the sequence started at Slough in 1931 and as such forms part of the longest continuous sequence of ionospheric data in the world.

[18] Having determined the average response of solar wind and geomagnetic parameters to the arrival of fast solar wind streams identified from east/west deflections in solar wind speed observed by the ACE spacecraft, the

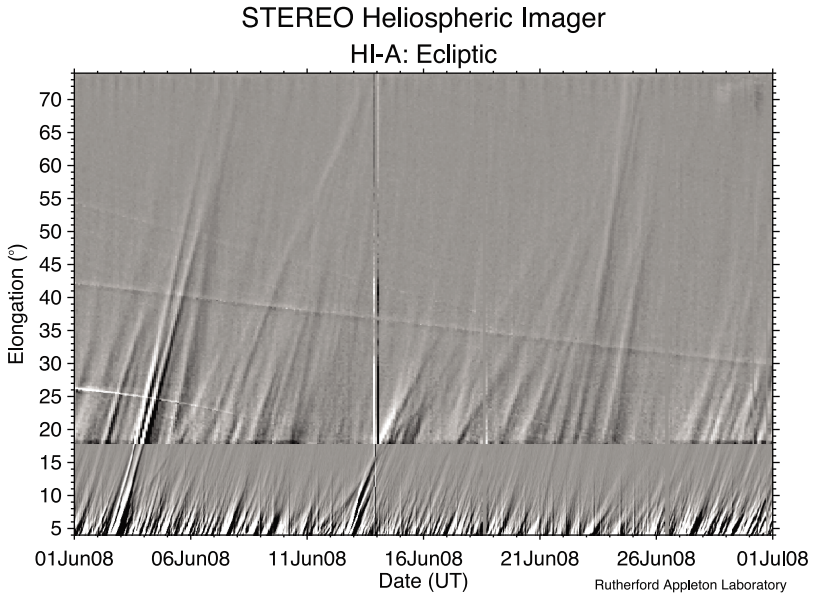

Figure 1. Plot of solar wind density as a function of elongation and time (a "J-map") constructed using slices along the ecliptic from images taken by the Heliospheric Imager on the STEREO-A spacecraft. This J-map has generated from the difference between consecutive images. In this way, faint propagated features in the solar wind are highlighted. White color represent an increase in intensity (and therefore electron concentration) while black represents a reduction in intensity. On these plots of elongation versus time, solar wind transients appear as features with a positive gradient.

analysis was repeated using arrival times predicted from STEREO/HI observations of the solar wind. Data from the STEREO-Ahead spacecraft were used for this study since the position of the two spacecraft during the first three years of the mission favored observation from HI-A of CIR-related transients ahead of their arrival at Earth.

[19] HI images were processed to form a map of solar wind density as a function of time (x axis) and elongation from the Sun (y axis). Such "j-maps" [*Davies et al.*, 2009] reveal solar wind transients moving out from the Sun as features with a positive gradient. An example of a typical j-map is shown in Figure 1. The curvature of these features is a function of the speed and direction of the transient relative to the observer. Features traveling away from the observer have an apparent deceleration while those traveling toward the observer have an apparent acceleration. For transients traveling at constant speed, this apparent acceleration is a geometrical artifact. From the vantage point of STEREO-A, transients associated with a single co-rotating stream appear as a family of curves that converge at large elongations [*Rouillard et al.*, 2008]. Coronal mass ejections also appear as features with positive gradients on such a plot but since they are most often isolated events, they most often appear as discrete features. Making the assumption that these features each travel at a constant speed and direction, the technique of *Rouillard et al.* [2008] was applied in order to estimate the speed and direction of each transient relative to the spacecraft. As the position of the spacecraft relative to Earth is known for all times, it was therefore possible to calculate the position of each transient relative to the Earth.

[20] While most of the bright features seen in the HI cameras to large elongations may be the result of small-scale transients entrained in co-rotating streams [*Rouillard et al.*, 2009, 2010a, 2010b], a significant fraction are associated with coronal mass ejections [*Davis et al.*, 2009; *Möstl et al.*, 2009] or CIRs interacting with CMEs [*Rouillard et al.*, 2010c]. In order to ensure that all the features used in this study were indeed co-rotating streams, all data within twelve hours of a CME entering the HI field of view were excluded from the current survey. In order to ascertain such times, we used observations of CMEs in the HI cameras identified by members of the citizen science project Solar Stormwatch (www.solarstormwatch.com). As part of this project, volunteers were asked to view movies of HI data and identify the time at which each CME entered the HI field of view. While CMEs and CIRs can look similar when viewed along the ecliptic in data products such as jmaps, they are very distinct in the HI images. CMEs appear as bright coherent "bubbles" of plasma that expand as they cross the field of view whereas plasma blobs associated with CIRs are much fainter, spatially constrained features that become more distinct as they propagate out from the Sun and become entrained at the stream interface. The Solar Stormwatch project uses the

philosophy introduced by the Zooniverse project [*Smith et al.*, 2012] in which the majority scaling decision of a large group of amateur volunteers has been shown to be as good as, if not better, than that of a single expert. This is certainly true for the CME times estimated by the members of Solar Stormwatch which compared very favorably with a small subset of start-times estimated by a single expert. A total of 193 CMEs were identified by Solar Stormwatch volunteers. By excluding times at which CMEs were seen in HI data, we are able to exclude the majority of CME effects from our study. This approach will exclude all but Earth-impacting CMEs that were not seen in the HI data (as occurred during the early stages of the STEREO mission when the spacecraft were close to the Earth and Earth-directed CMEs were difficult to see in the Heliospheric Imagers). The inclusion of the small number of such events will affect the ACE data but any superposed epoch analysis will be dominated by the effects of the much larger number of co-rotating streams because the mean of the measured values is taken for each time interval. By not considering CIR-associated transients occurring at the same times as CMEs, this study also excludes the effects of CMEs interacting with CIRs.

[21] Assuming that the remaining transients are associated with CIRs, the arrival time of the CIR at Earth (1 AU) was calculated for each transient from its radial velocity and transient-Sun-Earth angle, assuming that the streams co-rotated with the Sun with a period of 27 days. This equates to a change in angle of the co-rotating stream with respect to the Earth of around 13.3° per day. Several isolated transients are often associated with a single CIR, providing multiple estimates of the CIRs arrival at Earth. These HI-derived arrival times were then used to investigate the average behavior of solar wind parameters at Earth (as observed by the ACE spacecraft) and the consequent average response of the same geophysical parameters (i.e., in the same way as was done with ACE derived times).

3. Results

3.1. Identification of CIRs in in Situ Data From Near the L1 Point

[22] The average response of ACE solar wind parameters was found using a super-posed epoch study (also known as a "Chree analysis" or "compositing") around the time of arrival of 146 co-rotating streams, as estimated from ACE data (Figure 2). Figure 2a shows the average deflection in the east/west component of the solar wind derived from all the trigger events. This should, of course, be the sharpest curve as it is what defines the time = 0. At the arrival of the high-speed stream, the mean solar wind number density is enhanced from around 5 cm^{-3} to 20 cm^{-3} (Figure 2b), with the main peak having a full-width half maxima (FWHM) of around 10 h. At the same time, the mean solar wind speed (Figure 2c) is lower ahead of the events (-350 hrs < t < 0) but rises sharply near t = 0 to a peak of 540 km^{-1} and gradually returns to a slow solar wind speed of around 400 km^{-1} over a period of around 350 h (about 14.5 days). Meanwhile, the mean magnetic field strength is enhanced from 4 to 11 nT around t = 0 (Figure 2d) and, where a southward component of the field exists, this is enhanced from -1 to -4.5 nT on average (Figure 2e). Figure 2e constructed an average value for the north/south component of the magnetic field that used only those data with a southward (negative) component in each time bin. Since the sign of this component of the magnetic field can be either positive or negative, including all such data would generate an average response that would be near zero. Focusing on the southward component of the IMF is important as it is this which drives coupling with the Earth's magnetic field through magnetopause reconnection.

3.2. Terrestrial Response to CIRs Identified Using in Situ Data

[23] Having established that identifying the arrival of high-speed streams from their signatures in ACE data in this way leads to a strong and consistent response in other solar wind parameters, these times were then used to study the response of geophysical parameters (Figure 3).

[24] The Ap index (Figure 3a) was enhanced from 5 to 18 nT on average, starting at around 48 h ahead of the stream's arrival (at time = 0), peaking at time = 0 and continuing for several days. In fact Ap remains elevated above the pre-stream levels for about 6 days afterwards.

[25] The Dst index (Figure 3b) demonstrates a pre-stream enhancement from -5 to +10 nT (consistent with a compression of the magnetosphere due to the enhanced solar wind speed and density) followed by a sudden decrease to -21 nT within 24 h of the arrival of the stream (consistent with an enhancement in the equatorial ring current). The index slowly recovers to pre-stream levels over about 8 days.

[26] The mean cosmic ray flux was derived from the neutron monitor counting rate measured by the neutron monitor at Oulu (Figure 3c). It shows a slight rise ahead of the event arrival followed by steep drop around the arrival time of the high-speed stream, consistent with the increased shielding from cosmic rays afforded by the enhanced IMF at Earth. This decrease gradually recovers over the subsequent 200 h ($\sim$8 days). This behavior is consistent with the long-lived recurrent event studied by *Rouillard and Lockwood* [2007]. The changes in the geomagnetic field detected via the Dst index act to reduce the cut-off rigidities of cosmic rays at any one site [e.g., *Tyasto et al.*, 2008] and hence to increase the flux detected at the ground by the neutron monitor. From Figure 3 we see that the heliospheric shielding enhancement dominates over the weakening of the geomagnetic shield and cosmic ray fluxes impacting the atmosphere decrease.

[27] Finally, the response of the Earth's midlatitude ionosphere is represented by δfoF2 which is expressed as the deviation of the *F* region peak frequency from the monthly median value (Figure 3d). This was done in order to remove the otherwise dominant diurnal variation. It

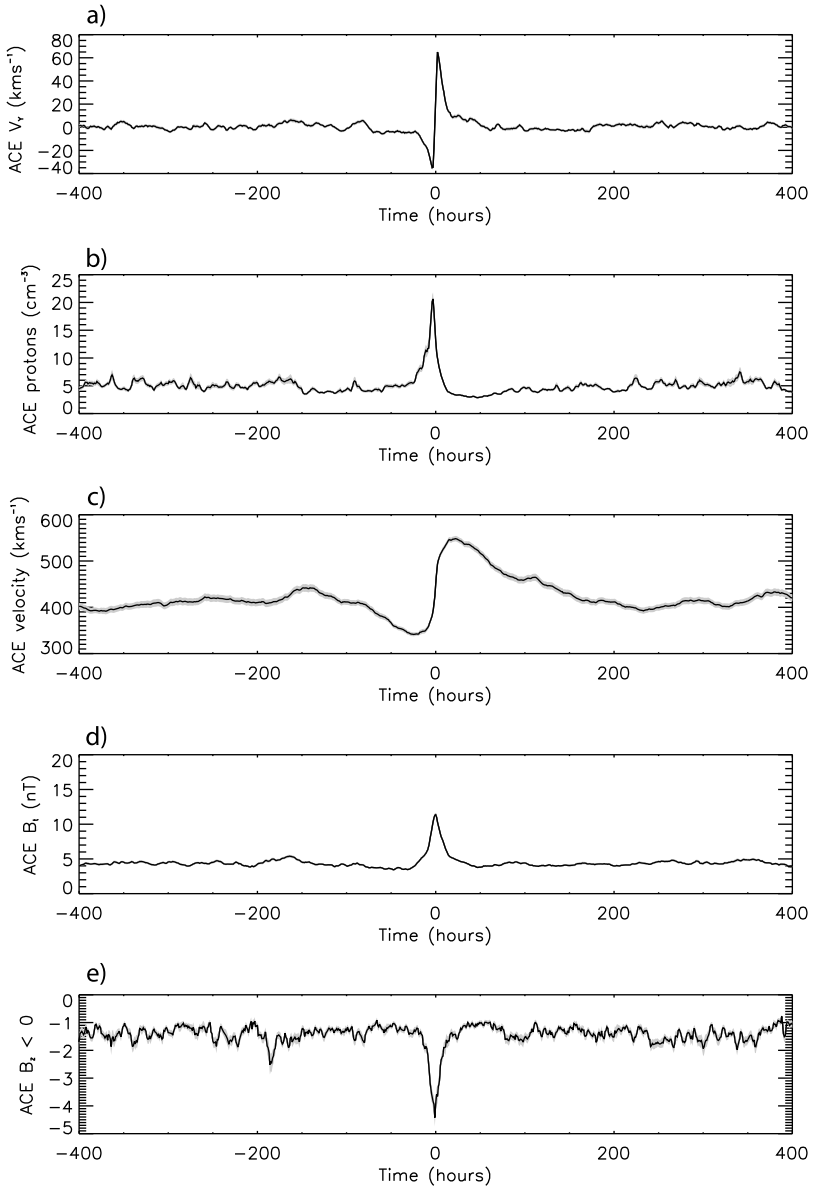

Figure 2. A superposed epoch analysis of solar wind data from the Advanced Composition Explorer spacecraft. The time of arrival of high-speed streams was estimated from a sudden increase in the E/W component of the solar wind velocity (Vy). These times were then used to construct the average response (black lines) to such streams of various solar wind parameters along with their mean errors (gray shaded region). These parameters are (a) mean E/W solar wind speed, (b) mean proton number density (cm^{-3}), (c) mean solar wind bulk velocity (km s^{-1}), (d) mean magnitude of the interplanetary magnetic field (nT), and (e) mean of the southward component of the interplanetary magnetic field (nT). A clear response in all parameters is seen to the arrival of high-speed solar wind streams (zero time offset).

can be seen that, on average, the *F* region peak frequency was enhanced by 0.4 MHz shortly after the arrival of a high-speed solar wind stream. Such an enhancement lasts around 10 h and thereafter the peak frequency is slightly lower than pre-stream condition for several days. While less dramatic, this is consistent with the response seen by *Denton et al.* [2009]. Such an initial enhancement of the ionosphere during a geomagnetic storm (known as the positive phase) is thought to result from transport of ionisation to greater altitudes where the loss-rate of ionisation is reduced. The mechanism for this could involve either meridional winds, enhanced electric fields or a

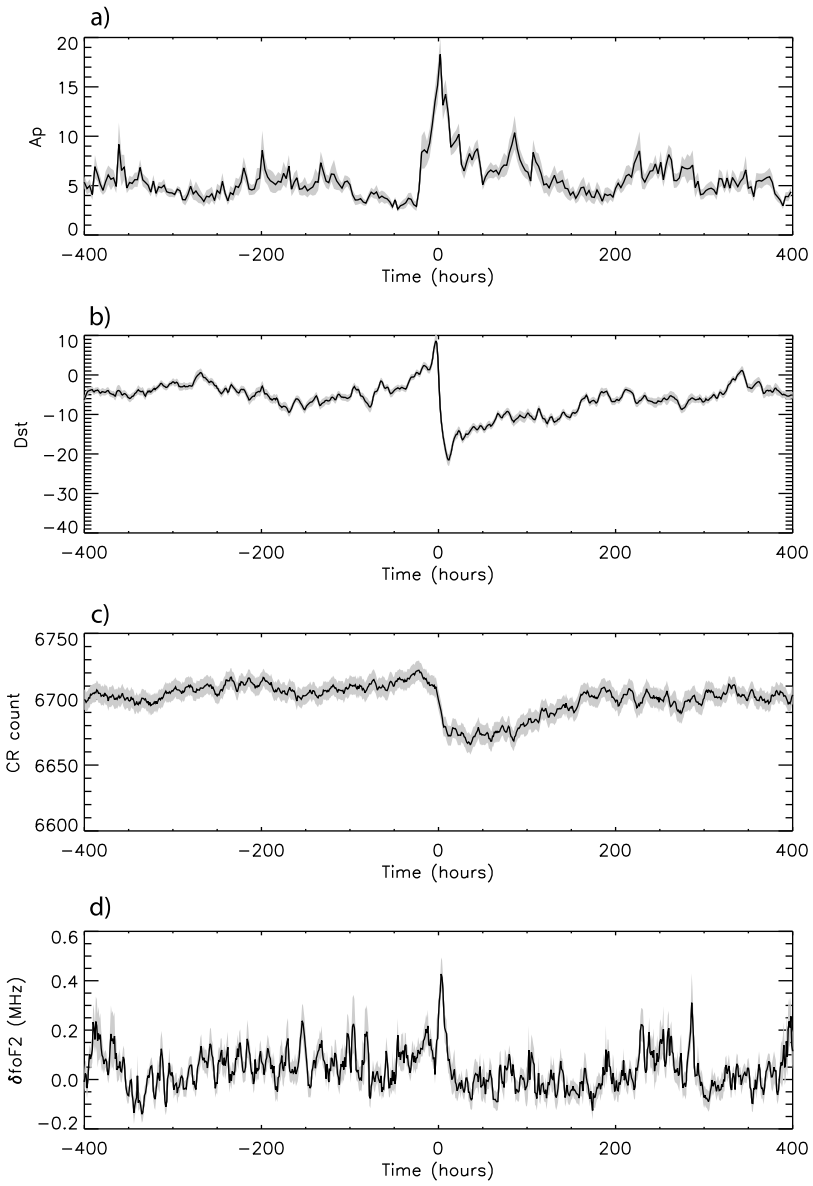

Figure 3. The average response (black lines) along with the mean error (gray shaded region) of various geophysical parameters to the arrival of the same solar wind streams identified from ACE data and used in Figure 2. These are (a) mean Ap geomagnetic index, (b) mean Dst index, (c) mean cosmic ray count at Oulu in Finland, and (d) mean ionospheric *F* region critical frequency at Chilton in the UK (presented as a deviation from the monthly median). All parameters show a clear response to the arrival of high-speed solar wind streams at zero time offset.

combination of the two [*Balan et al.*, 2010]. Currents flowing in the high-latitude *F* region during times of geomagnetic activity heat the plasma through frictional drag with the neutral thermosphere. Since the ion recombination rates are temperature dependant, this frictional heating leads to a temporary but dramatic decrease in ionospheric concentration at high latitudes. If the period of frictional heating is prolonged, molecular rich air upwells from the lower thermosphere which also enhances the loss rate of ionisation. Such changes to the thermospheric composition lead to ionospheric depletions that can last for several days and affect the entire planet as this molecular rich air is transported via global atmospheric circulation patterns [e.g., *Fuller-Rowell et al.*, 1994].

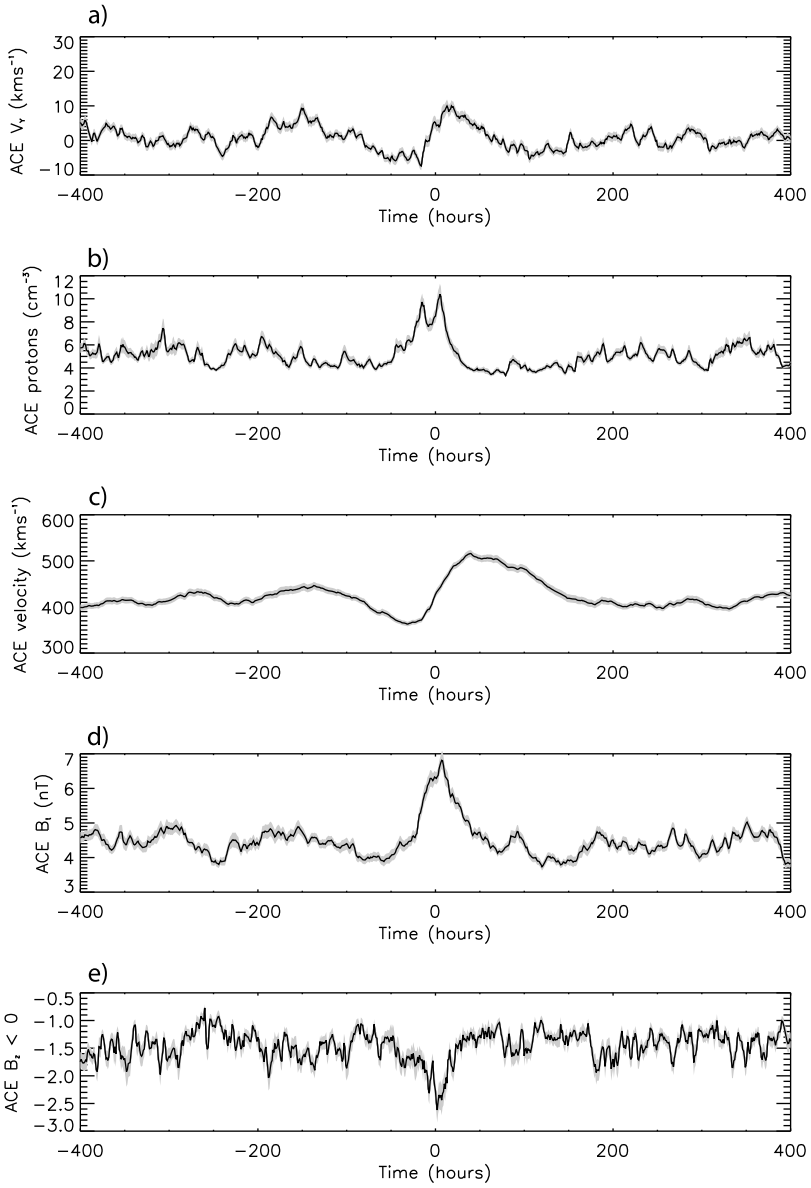

Figure 4. This plot is similar to Figure 2 except that the arrival times of high-speed solar wind streams at Earth were estimated by adding the 27 day solar rotation time to each in situ observation. While the response of all parameters is still clear, they are much reduced in amplitude and broadened in time resulting from the uncertainties involved in assuming that high-speed streams did not evolve over the course of a solar rotation.

[28] Having used in situ spacecraft data to accurately determine the arrival of high-speed solar wind streams at Earth, Figures 2 and 3 show that there are clear responses in the average behavior of both solar wind and selected geomagnetic parameters.

3.3. Prediction of CIRs and Their Effects Using in Situ Data

[29] Current predictions of the arrival of high-speed solar wind streams at Earth use the solar rotation rate to predict the arrival of the same stream at Earth 27 days after it was first observed in situ. This assumes that each high-speed stream exists for 27 days or longer and does not change significantly between rotations. If a new stream emerged during the rotation, such a stream would not be predicted by this technique though observation of coronal hole structures would offer some clues. To test the performance of such an assumption, 27 days were added to the times of high-speed streams at Earth identified in section 2, and these modified times were used in a

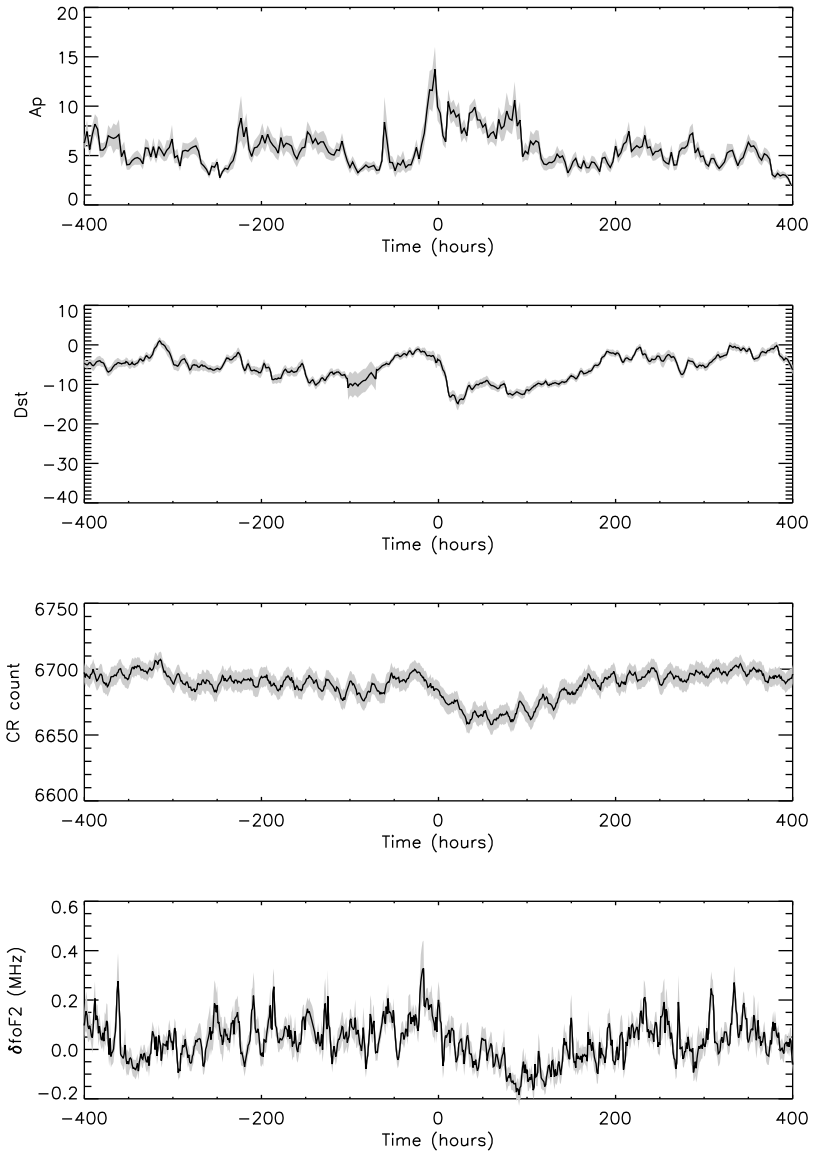

Figure 5. The response of geomagnetic parameters to the arrival of the same high-speed solar wind streams predicted from in situ data used in Figure 4. There are clear responses in all parameters to the arrival of the high-speed solar wind streams. The reduced amplitude and greater width of such features compared with those presented in Figure 3 result from the uncertainities in the predicted arrival times of high-speed streams at Earth.

second superposed epoch analysis to investigate the accuracy of such a prediction. The results are shown in Figures 4 and 5 (the axes of these plots differ from those in Figures 2 and 3 since the features are less prominent). It can be seen that when in situ data are used to predict the arrival of high-speed streams at Earth, the average response is more uncertain. While there are still clear responses in all parameters, they are all broadened over time and have smaller amplitudes, resulting from uncertainties in their arrival times and changes that occur to each stream within the 27 day rotation rate of the Sun.

3.4. Identification of CIRs and Their Effects Using Remote Sensing Data From STEREO

[30] The above analyses were repeated using the predicted arrival times of high speed solar wind streams at Earth estimated from STEREO/HI observations. The accuracy in determining the direction and speed of such streams varies according to the elongation range over which each CIR-associated transient could be observed. Since the speed and direction of these streams are used to predict the arrival of each high-speed stream at Earth,

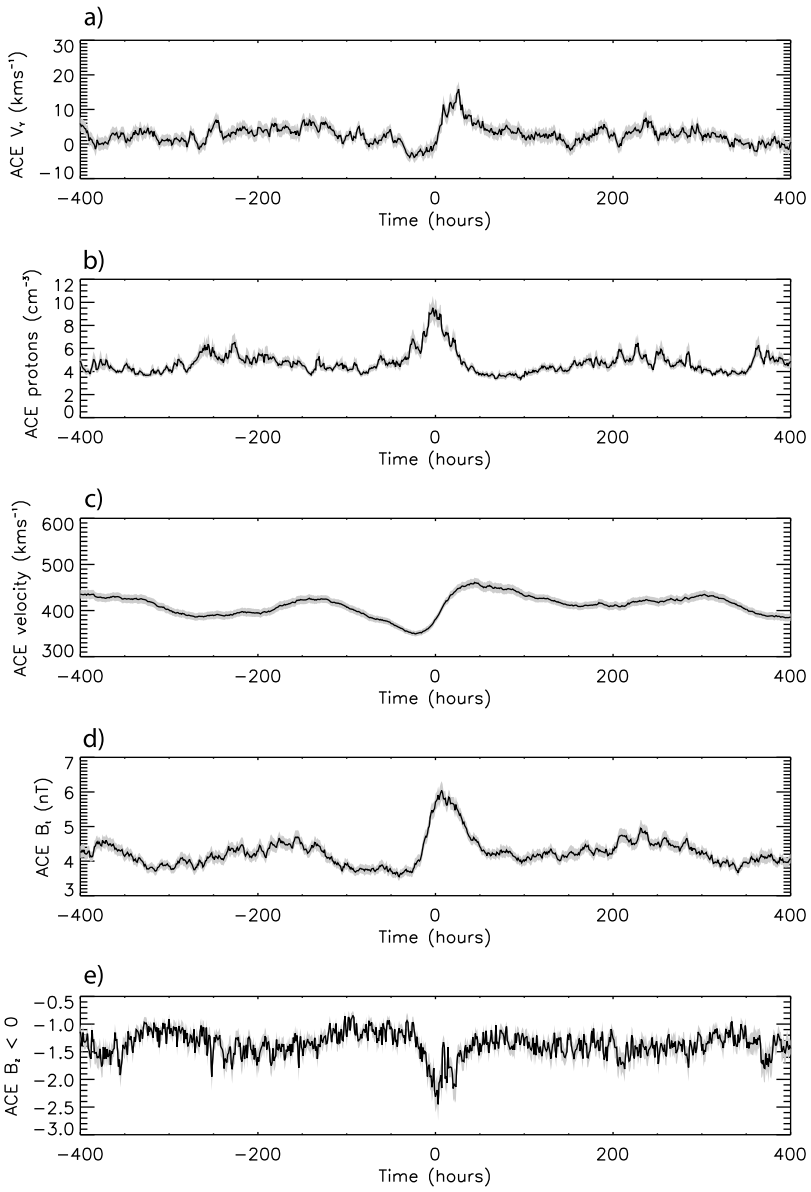

Figure 6. This plot is similar to Figure 4 except that the arrival times of high-speed solar wind streams at Earth were estimated from observations of solar wind transients observed by the STEREO-A Heliospheric Imager. Again, the solar wind as observed by ACE shows a clear response in all parameters shown around a zero time offset. The time-broadening of the various responses compared with those shown in Figure 4 gives an indication of to the relative uncertainties in the two sets of timing pulses (from ACE Vy and STEREO/HI images).

their associated uncertainties can be used to estimate the uncertainty in the arrival time of such a stream at Earth. For those transients that can only be tracked over a relatively short elongation range, the associated uncertainties can be large. Only those high-speed streams whose arrival time at Earth could be estimated with an uncertainty of less than a day were used in this study. Figure 6 presents the average response of solar wind parameters to the arrival of high-speed streams estimated from 244 observations of CIR-associated transients while Figure 7 shows the average response of selected geophysical parameters (corresponding to Figures 4 and 5 for the events predicted using in situ data). Figure 6 shows that the interplanetary parameters behave in the same way as in Figure 4. There is a marked change in the E/W component of the solar wind (Figure 6a), an enhancement in the proton density, solar wind speed, and magnetic field strength (Figures 6b–6d). Once again, for those events in which there was a

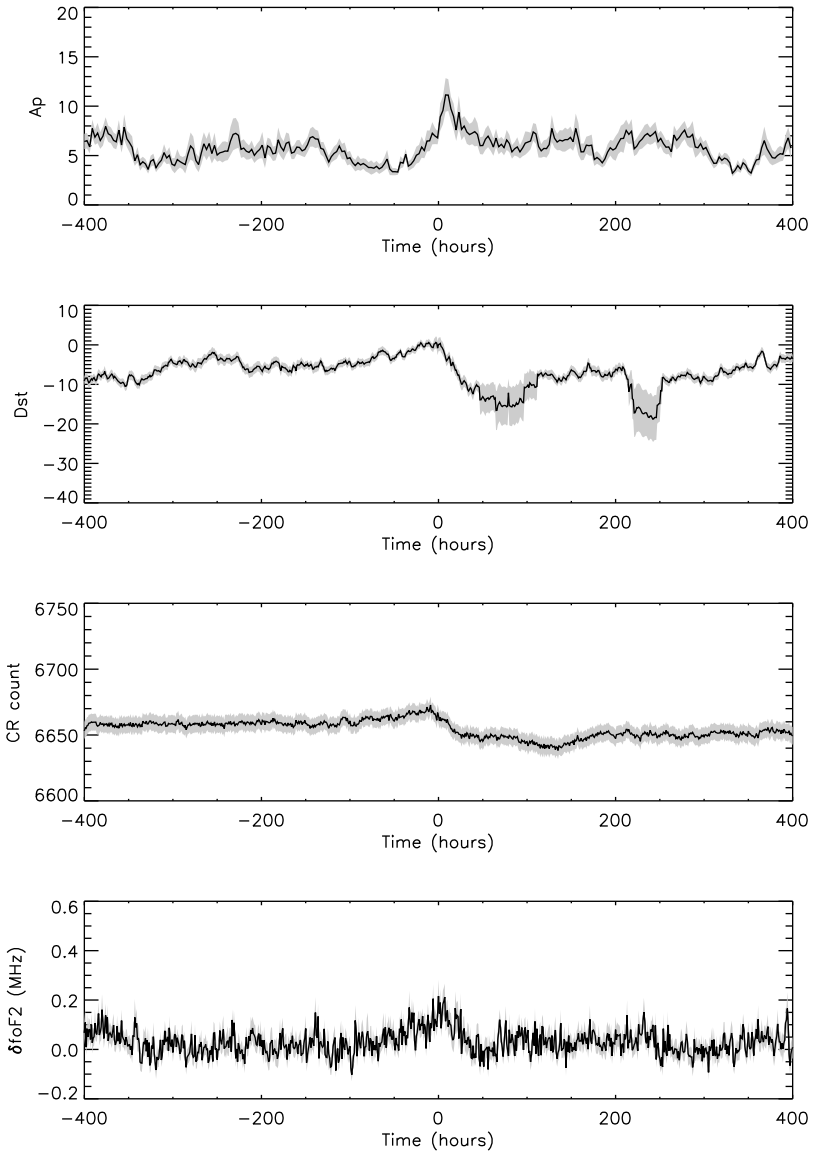

Figure 7. The response of geomagnetic parameters to the arrival of the same high-speed solar wind streams identified from STEREO-HI data as used in Figure 6. The geomagnetic parameters are presented in the same way as for Figure 5. Again there are clear responses in all parameters to the arrival of the high-speed solar wind streams.

southward component of the IMF, this component was enhanced (Figure 6e). While there is little difference between Figures 4 and 6, the peak velocity and magnetic field strength predicted from the STEREO observations are slightly less sharp for the remotely sensed events due to the uncertainties in predicting the arrival of high speed streams at Earth from STEREO/HI data. The terrestrial responses in Figure 7 also show responses similar to those presented in Figure 5. Again some parameters are slightly less well defined in Figure 7 which used STEREO data to predict the onset of the high-speed streams. The response of Dst in this and subsequent plots is relatively noisy since preliminary data were used.

[31] It is clear therefore that it is possible to track co-rotating streams through observation of CIR-associated transients in STEREO-HI data and successfully estimate their arrival at Earth. Such average responses are similar to those predicted using in situ identification of such streams, there are a few minor differences. Taking the proton concentrations as an example, the peak at time = 0 obtained using ACE data for the timing pulse (Figure 4b) peaks at 10 cm^{-3} and has a FWHM of around 38 h. This compares with a peak of 9.5 cm^{-3} and a FWHM of

~51 h when considering the peak derived when using STEREO HI data to estimate the arrival of high-speed streams (Figure 6b). This gives some indication of the uncertainty in estimating the arrival of solar wind streams at Earth using STEREO data compared with estimates predicted using in situ data. The advantage of using STEREO-HI images is that any new streams that emerge during the solar rotation can be identified and used to estimate the arrival of that solar wind stream several days in advance of its arrival at Earth. If such a stream were identified from ACE data alone, the warning is only the L1-to-Earth propagation delay which typically varies between 20 min and an hour.

[32] In order to investigate whether the use of STEREO-HI data can actually provide a useful prediction of the arrival of high-speed streams at Earth, the data were further restricted to include only those streams that had yet to reach Earth and for which the stream-Sun-Earth angle was greater than 13.3° (i.e., the events are detected over 24 h before their predicted arrival at Earth). Thus we repeated the superposed-epoch analysis based on this limited set of 99 HI-derived times. The results of this analysis are shown in Figures 8 and 9. Once again there are clear responses in all solar wind parameters which are slightly more well-defined than those shown in Figures 6 and 7. This could be due to an optimized viewing geometry for such events. The response of the geophysical parameters is once again clear although the reduction in the number of events has led to a noticeable increase in the variability of each averaged data set compared with Figure 7, with the ionospheric enhancement (Figure 9d) being the least clear.

[33] This analysis was repeated for lead times of 2, 3 and 4 days (stream-Sun-Earth angles of 26.6°, 39.9° and 55.2°). While the results from these analyses are not shown, the solar wind and geophysical responses were clear throughout, becoming noisier in proportion to the rise in the standard errors in the means as the number of samples in each study reduced.

[34] The evolving position of the STEREO spacecraft relative to the Earth throughout the mission means that while the previous analysis demonstrates the potential to use heliospheric images like those from STEREO/HI to predict the arrival of high-speed streams at Earth, it does not represent the case for an operational space-weather monitor located at a fixed distance ahead of Earth in its orbit. For such a mission, it would be desirable to be sufficiently far from the Sun-Earth line that the speed and direction of Earth-directed CMEs could be determined while also being sufficiently close to Earth to provide advanced warning of the arrival of high-speed solar wind streams through observations of CIR-associated transients propagating along solar longitudes well ahead of their arrival at Earth. In order to investigate the validity of such a mission, the data were further restricted to include those events which were observed over 24 h in advance of their arrival at Earth (as above) but also for which the earth-Sun-spacecraft angle exceeded 40°. Such a position was chosen somewhat arbitrarily and would need to be optimized but STEREO has seen at least one Earth-impacting CME from such a position [*Davis et al.*, 2009] and such an example serves to demonstrate the feasibility of a mission to predict both CMEs and high-speed streams. The results are presented in Figures 10 and 11 (for interplanetary and terrestrial parameters, respectively). Encouragingly for the 91 events in this study the average responses of solar wind parameters are not dissimilar to those for the previous subset (although they are slightly noisier due to the small reduction in samples). Similarly, the average response is still visible in all the geophysical parameters although, again, with increased levels of background noise due to the reduced number of samples.

4. Discussion and Future Work

[35] One question raised by the analysis presented in section 3 is how efficiently we can track CIR-associated transients (and therefore high-speed streams) in STEREO data. Further analysis is required to estimate the proportion of solar wind streams identified in the STEREO-HI data as compared with those measured in situ by spacecraft such as ACE. For such a stream to become visible in the HI cameras requires plasma to be entrained at the CIR interface where it becomes concentrated. From a simple comparison of the number of events seen by ACE and HI-A in this study (146 rapid changes in solar wind V_y component compared with 244 CIR-associated transients) it would seem that there is a large overlap between the two sets but a more detailed analysis which linked individual events would be required in order to determine the plasma concentration necessary for a CIR-associated transient to be detected in HI images. Such an analysis may also reveal how the speed and trajectory of a transient influences its visibility in HI images.

[36] While this study has demonstrated the potential for using HI images to predict the arrival of high-speed solar wind streams at Earth, there will undoubtedly be ways of improving on the analysis. In our study we have used "differenced" images to produce the j-maps. This has the advantage of revealing faint propagating features with sharp boundaries, however, they also introduce some ambiguity into the exact timing of a trace. The clearest part of a transient feature in a j-map image is the interface between the light (enhanced) and black (depleted) sections of a trace. Such boundaries were used to track each transient since they are the most clearly defined but they do not represent the leading edge of the CIR density front. As such they will lead to a small (late) offset in the predicted arrival times at Earth. In addition, the arrival time of the high-speed stream obtained from the in situ data has been based on a change in the solar wind Vy component while the arrival time of the high-speed stream from the STEREO/HI data was based on the plasma density enhancement. A comparison of the average proton densities in Figures 2a and 4a shows a slight offset in

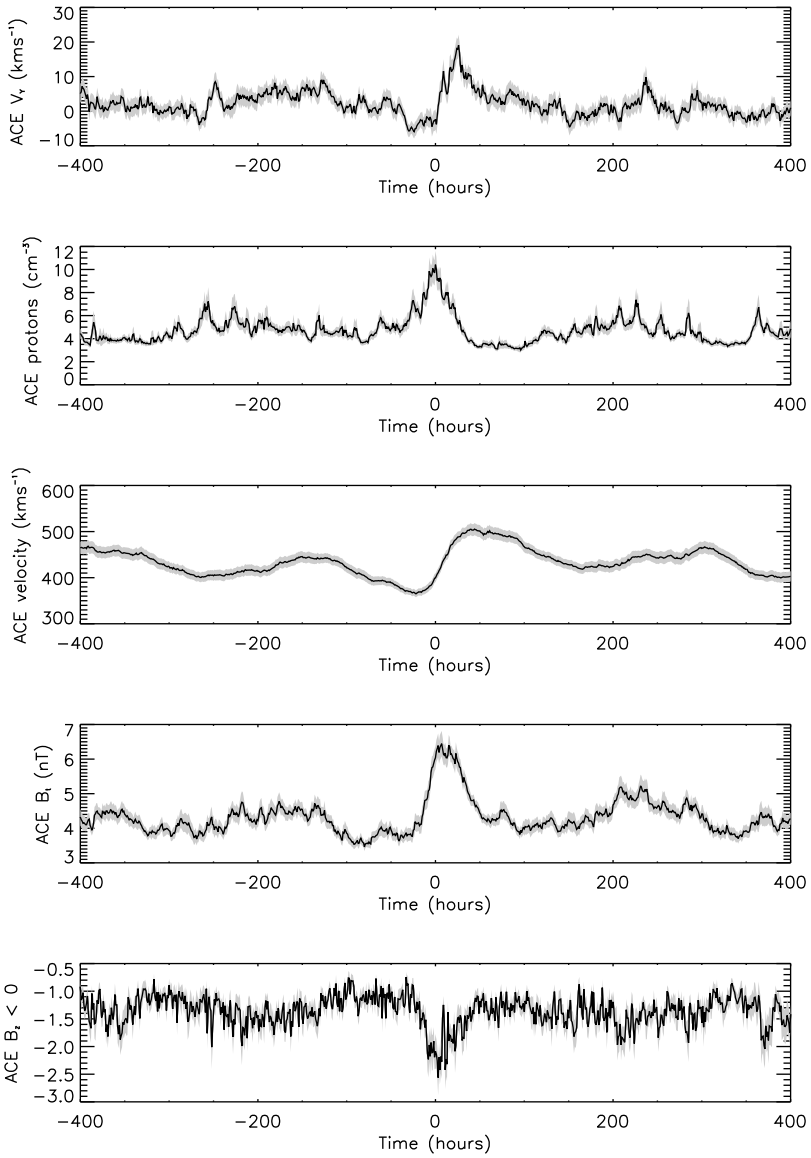

Figure 8. Average behavior of solar wind parameters measured by the ACE spacecraft in response to the arrival of a subset of high-speed solar wind streams identified in the STEREO HI data and observed at least one day ahead of their arrival at Earth. Such a subset provides confidence that the solar wind transients observed in the data are observed with sufficient accuracy that their arrival at Earth could be forecast at least 24 h ahead.

their arrival times which may result from a combination of these assumptions.

[37] The tracking of the CIR-associated transients used in this study has assumed that they propagate at a constant speed and direction and that these observations act as an exact proxy to the onset of high-speed flow. While the clear average response in in situ solar wind data at the estimated arrival time demonstrates that this approximation is valid, a more comprehensive analysis of the velocity profile of such transients as they become entrained at the stream interface may improve on the measured uncertainties.

[38] Another limitation of the current analysis is that the time-elongation profiles for features in the j-map traces were all traced from the J-map manually. Previous studies on individual CME traces scaled in this way [*Davis et al.*, 2010] revealed that it was preferable to scale each event multiple times to limit the effect of any random errors introduced by manual scaling. For this current study, it was not possible to scale each event many times due to the large number of events being studied. As such errors are independent and random between events they are unlikely to have a cumulative effect other than to broaden

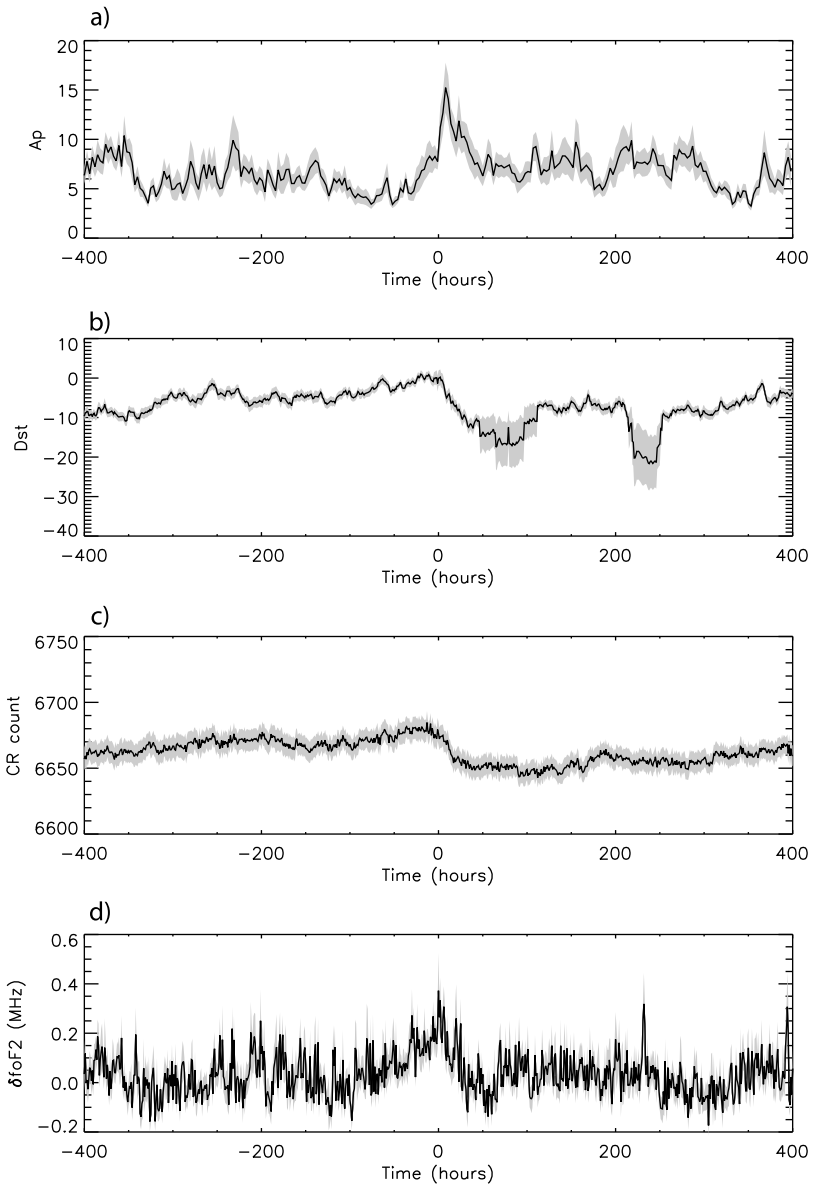

Figure 9. The average response of geophysical parameters to the subset of high-speed solar wind streams indentified in the STEREO-HI data and observed at least one day ahead of their arrival at Earth. Again it can be seen that all parameters show a clear response to the arrival of high-speed solar wind streams, with the broadening of the features compared with Figure 5 demonstrating the uncertainties associated with such a forecast.

any averaged features. A process for automatically identifying such traces is clearly desirable but the complexity of this problem is beyond the scope of this paper.

[39] The arrival times at Earth and the ACE spacecraft were considered to be the same for events tracked in STEREO images. Accounting for the propagation time between ACE and Earth will introduce a small (∼40 min) systematic error in the arrival times at ACE, broadened by the observed spread in velocities. Since the uncertainties in predicted arrival time are often significantly larger than this, such a refinement would have a very minor effect on the mean response of the ACE parameters presented here.

[40] Finally, this study has used data from the HI instrument on the STEREO-A spacecraft since this is orbiting ahead of the Earth and CIR-associated transients approaching Earth are therefore within the field of view of the spacecraft. In principle, this analysis could equally have been done with data from the STEREO-B spacecraft but in order for any CIR-related transients to have been

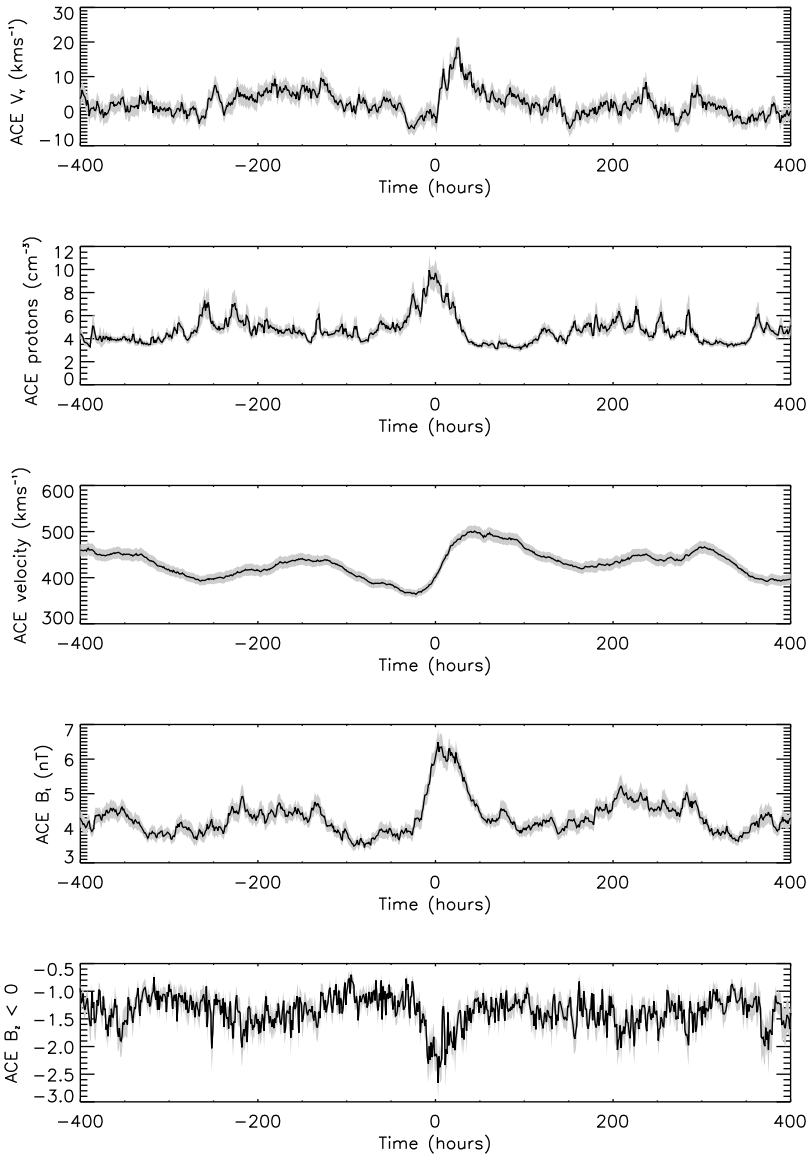

Figure 10. The average behavior of solar wind parameters measured by the ACE spacecraft in response to the arrival of a subset of high-speed solar wind streams identified in the STEREO-HI data and observed at least one day ahead of their arrival at Earth from a spacecraft positioned more than 40 degrees ahead of the Earth along the ecliptic. Such a subset represents data from the position of an operational space-weather observatory. Once again, there is a clear response in all the solar wind parameters shown.

observed before their arrival at Earth, the spacecraft-Sun-Earth angle would need to have been much larger, requiring data from later in the mission.

[41] Predicting the arrival of high-speed streams at Earth from a spacecraft separated from Earth by many degrees in solar longitude introduces the implicit assumption that the nature of the solar wind does not change significantly over such distances. When solar wind velocities measured by both the ACE and STEREO spacecraft were correlated as a function of the spacecraft separation, it was found that the phase lag at maximum correlation between the two data sets decreased approximately linearly as the longitude difference between the ACE and STEREO spacecraft increased [*Riley et al.*, 2010]. Modeling work suggested that deviations from this trend were due to spatial inhomogeneities in the plasma or to the temporal evolution of streams. A complementary study [*Opitz et al.*, 2009] separated the temporal and spatial variability of the solar wind to show that there was a correlation of 0.95 for a time lag of 0.5 days which decrease to a correlation of 0.85 as the time

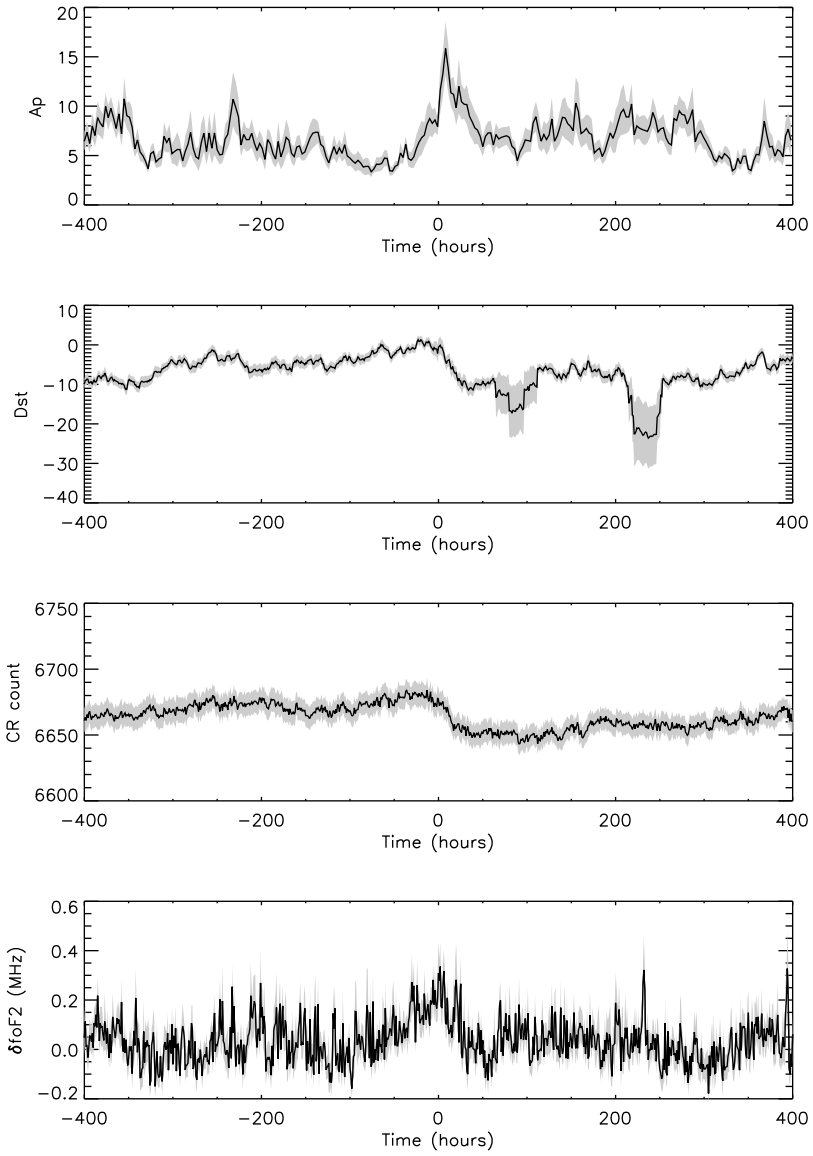

Figure 11. The response of geomagnetic parameters to the subset of solar wind streams used in Figure 10. A clear response in all geomagnetic parameters can be seen, with the temporal broadening of each response compared with Figure 5 demonstrating the relative uncertainties associated with each technique.

lag increased to 2 days. *Jian et al.* [2009] studies three CIR structures in depth from several spacecraft and concluded that the observed variability across a stream interface was similar for spacecraft separated by 7° and 42° in solar longitude. They concluded that such variability was the result of both spatial and temporal variability. Predicting the arrival of solar wind streams at Earth can never be perfect and a compromise has to be reached between large spatial and temporal separations which would provide an early yet less accurate forecast and smaller separations which, while more accurate, will provide less warning. In practice, such a warning system will benefit from the early prediction of an approaching high-speed stream, the accuracy of which can be refined as it approaches. Such warnings could be provided by an in situ monitor lagging behind the Earth in its orbit or an imaging system orbiting ahead of the Earth. Both options have their merits. Experience from the STEREO mission has shown that an imaging system observing the Sun-Earth line from a position behind the Earth is more vulnerable to offsets caused by the impact by micro-meteoroids [*Davis et al.*, 2012] while in situ solar wind measurements are clearly more useful if made in advance of their arrival at Earth. The current study has shown that an imaging system

orbiting ahead of the Earth would, on average, be able to predict the arrival of high-speed solar wind streams at Earth as effectively as predictions made from in situ measurements along the Sun-Earth line. Such an imaging system would also be able to track the speed and direction of CMEs, providing coverage of both phenomena from a single instrument.

[42] The data used in this study were the high-resolution science data that are not available in real-time. STEREO also broadcasts a near real-time "space-weather beacon" which has been used to make real-time predictions of the arrival of CMEs at Earth [*Davis et al.*, 2011]. Very few, if any, CIR-associated transients are visible in these images since they are of reduced-resolution and lossily compressed due to the telemetry constraints of such a mission. If HI images are to be used to predict the arrival of high-speed solar wind streams at Earth in real-time, provision will need to be made to return higher-resolution data in the space-weather beacon. Such a data stream could potentially be made to fit within the telemetry budget by returning only selected portions of the images (along the ecliptic) or through onboard processing of the data.

5. Conclusions

[43] We have shown that STEREO-HI data can be used to successfully estimate the arrival of high-speed solar wind streams at Earth through observation of enhanced regions of plasma density entrained at the stream interface of a CIR. Not only this, but we show that there is a viable predictive capability. This result appears to contradict the results of *Williams et al.* [2011] who investigated a small number of case-studies. Furthermore, our results demonstrate the potential to predict the response of solar wind and geomagnetic parameters and such information is useful to forecasters wishing to include the effects of high-speed solar wind streams in their models, not only to estimate the response of the geomagnetic system but also in characterizing the background solar wind in models used to forecast the propagation of CMEs to Earth.

[44] One striking difference between our analysis and that of *Denton et al.* [2009] is the lack of a pronounced and extended reduction in ionospheric concentration after the initial enhancement as the magnetosphere was compressed by the arrival of the high-speed stream (at time = 0). It would be interesting to investigate whether this was due to the different number of samples in each study or whether it indicates that the ensuing substorms were either weaker or absent during most of the events observed during the STEREO era as compared with the extended data set used by *Denton et al.* [2009]. If the latter proves to be the case, it is perhaps unsurprising when viewed in the context of the recent extended solar minimum which has led to historically low values of solar wind proton density and IMF.

[45] **Acknowledgments.** The U.K. STEREO-HI team is funded by the U.K. Space Agency. The STEREO-HI and geophysical data are hosted by the U.K. Solar System data center (www.ukssdc.ac.uk). We thank the ACE SWEPAM and MAG instrument teams and the ACE Science Center for providing the ACE data. Solar Stormwatch is a collaborative project between the Galaxy Zoo team, the Royal Observatory Greenwich, and the Science and Technology Facilities Council. The Zooniverse is supported by The Leverhulme Trust. This article includes data analysis that has been made possible by the participation of more than 15,000 volunteers in the Solar Stormwatch project (https://www.solarstormwatch.com/authors).

References

Arge, C. N., and V. J. Pizzo (2000), Improvement in the prediction of solar wind conditions using near-real time solar magnetic field updates, *J. Geophys. Res.*, *105*(A5), 10,465–10,479, doi:10.1029/1999JA000262.

Balan, N., K. Shiokawa, Y. Otsuka, T. Kikuchi, D. V. Lekshmi, S. Kawamura, M. Yamamoto, and G. J. Bailey (2010), A physical mechanism of positive ionospheric storms at low latitudes and midlatitudes, *J. Geophys. Res.*, *115*, A02304, doi:10.1029/2009JA014515.

Billings, D. E. (1966), *A Guide to the Solar Corona*, Academic, New York.

Borovsky, J. E., and M. H. Denton (2006), Differences between CME-driven storms and CIR-driven storms, *J. Geophys. Res.*, *111*, A07S08, doi:10.1029/2005JA011447.

Davies, J. A., R. A. Harrison, A. P. Rouillard, N. R. Sheeley Jr., C. H. Perry, D. Bewsher, C. J. Davis, C. J. Elyes, S. Crothers, and D. S. Brown (2009), A synoptic view of solar transient evolution in the inner heliosphere using the Heliospheric Imagers on STEREO, *Geophys. Res. Lett.*, *36*, L02102, doi:10.1029/2008GL036182.

Davis, C. J., J. A. Davies, M. Lockwood, A. P. Rouillard, C. J. Eyles, and R. A. Harrison (2009), Stereoscopic imaging of an Earth-impacting solar coronal mass ejection: A major milestone for the STEREO mission, *Geophys. Res. Lett.*, *36*, L08102, doi:10.1029/2009GL038021.

Davis, C. J., J. Kennedy, and J. A. Davies (2010), Assessing the accuracy of CME speed and trajectory estimates from STEREO observations through a comparison of independent methods, *Sol. Phys.*, *263*(1–2), 209–222, doi:10.1007/s11207-010-9535-2.

Davis, C. J., et al. (2011), A comparison of space weather analysis techniques used to predict the arrival of the Earth-directed CME and its shockwave launched on 8 April 2010, *Space Weather*, *9*, S01005, doi:10.1029/2010SW000620.

Davis, C. J., et al. (2012), The distribution of interplanetary dust between 0.96 and 1.04 AU as inferred from impacts on the STEREO spacecraft observed by the Heliospheric Imagers, *Mon. Not. R. Astron. Soc.*, in press.

Denton, M. H., T. Ulich, and E. Turunen (2009), Modification of midlatitude ionospheric parameters in the F2 layer by persistent high-speed solar wind streams, *Space Weather*, *7*, S04006, doi:10.1029/2008SW000443.

Eyles, C. J., et al. (2009), The Heliospheric Imagers onboard the STEREO Mission, *Sol. Phys.*, *254*, 387–445, doi:10.1007/s11207-008-9299-0.

Fuller-Rowell, T. J., M. V. Codrescu, R. J. Moffett, and S. Quegan (1994), Response of the thermosphere and ionosphere to geomagnetic storms, *J. Geophys. Res.*, *99*, 3893–3914, doi:10.1029/93JA02015.

Hapgood, M. A. (1993), A double solar cycle in the 27 day recurrence of geomagnetic activity, *Ann. Geophys.*, *11*, 248–253.

Hapgood, M. (2011), Towards a scientific understanding of the risk from extreme space weather, *Adv. Space Res.*, *47*, 2059–2072, doi:10.1016/j.asr.2010.02.007.

Hapgood, M. A., M. Lockwood, G. A. Bowe, D. M. Willis, and Y. K. Tulunay (1991), Variability of the interplanetary medium at 1 a.u. over 24 years: 1963–1986, *Planet. Space Sci.*, *39*(3), 411–423, doi:10.1016/0032-0633(91)90003-S.

Howard, R. A., et al. (2008), Sun Earth Connection Coronal and Heliospheric Investigation (SECCHI), *Space Sci. Rev.*, *136*, 67–115, doi:10.1007/s11214-008-9341-4.

Jian, L., K. Russell, C. T. Luhmann, J. G. Galvin, A. B. Mac, and P. J. Neice (2009), Multi-spacecraft observations: Stream interactions and associated structures, *Sol. Phys.*, *259*, 345–360, doi:10.1007/s11207-009-9445-3.

Kahler, S. W., and D. F. Webb (2007), V arc interplanetary coronal mass ejections observed with the Solar Mass Ejection Imager, *J. Geophys. Res.*, *112*, A09103, doi:10.1029/2007JA012358.

Kaiser, M. L., T. A. Kucera, J. M. Davilla, O. C. St. Cyr, M. Guhathakurta, and E. Christian (2008), The STEREO mission: An introduction, *Space Sci. Rev.*, *136*, 5–16, doi:10.1007/s11214-007-9277-0.

Liu, Y., J. A. Davies, J. G. Luhmann, A. Vourlidas, S. D. Bale, and R. P. Lin (2010), Geometric triangulation of imaging observations to track coronal mass ejections continuously out to 1 AU, *Astrophys. J.*, *710*, L82, doi:10.1088/2041-8205/710/1/L82.

Lugaz, N., A. Vourlidas, and I. I. Roussev (2009), Deriving the radial distances of wide coronal mass ejections from elongation measurements in the heliosphere—Application to CME-CME interaction, *Ann. Geophys.*, *27*, 3479, doi:10.5194/angeo-27-3479-2009.

McComas, D. J., H. A. Elliott, N. A. Schwadron, J. T. Gosling, R. M. Skoug, and B. E. Goldstein (2003), The three-dimensional solar wind around solar maximum, *Geophys. Res. Lett.*, *30*(10), 1517, doi:10.1029/2003GL017136.

McPherron, R. L., G. Siscoe, and C. N. Arge (2004), Probabilistic forecasting of the 3-h Ap index, *IEEE Trans. Plasma Sci.*, *32*, 1425, doi:10.1109/TPS.2004.833387.

Möstl, C., C. J. Farrugia, M. Temmer, C. Miklenic, A. M. Veronig, A. B. Galvin, M. Leitner, and H. K. Biernat (2009), Linking remote imagery of a coronal mass ejection to its in situ signatures at 1 AU, *Astrophys. J.*, *705*, L180–L185, doi:10.1088/0004-637X/705/2/L180.

Opitz, A., et al. (2009), Temporal evolution of the solar wind bulk velocity at solar minimum by correlating the STEREO A and B PLASTIC measurements, *Sol. Phys.*, *256*, 365–377, doi:10.1007/s11207-008-9304-7.

Parker, E. N. (1963), *Interplanetary Dynamical Processes*, Wiley-Intersci., New York.

Pizzo, V. J. (1991), The evolution of corotating stream fronts near the ecliptic plane in the inner solar system: 2. Three-dimensional tilted-dipole fronts, *J. Geophys. Res.*, *96*, 5405–5420, doi:10.1029/91JA00155.

Riley, P., J. A. Linker, and Z. Mikić (2001), An empirically driven global MHD model of the solar corona and inner heliosphere, *J. Geophys. Res.*, *106*, 15,889–15,901, doi:10.1029/2000JA000121.

Riley, P., J. Luhmann, A. Opitz, J. A. Linker, and Z. Mikic (2010), Interpretation of the cross-correlation function of ACE and STEREO solar wind velocities using a global MHD model, *J. Geophys. Res.*, *115*, A11104, doi:10.1029/2010JA015717.

Rouillard, A. P., and M. Lockwood (2007), The latitudinal effect of corotating interaction regions on galactic cosmic rays, *Sol. Phys.*, *245*, 191–206, doi:10.1007/s11207-007-9019-1.

Rouillard, A. P., et al. (2008), First imaging of corotating interaction regions using the STEREO spacecraft, *Geophys. Res. Lett.*, *35*, L10110, doi:10.1029/2008GL033767.

Rouillard, A. P., et al. (2009), A multispacecraft analysis of a small-scale transient entrained by solar wind streams, *Sol. Phys.*, *256*, 307–326, doi:10.1007/s11207-009-9329-6.

Rouillard, A. P., et al. (2010a), Intermittent release of transients in the slow solar wind: 1. Remote sensing observations, *J. Geophys. Res.*, *115*, A04103, doi:10.1029/2009JA014471.

Rouillard, A. P., et al. (2010b), Intermittent release of transients in the slow solar wind: 2. In situ evidence, *J. Geophys. Res.*, *115*, A04104, doi:10.1029/2009JA014472.

Rouillard, A. P., B. Lavraud, N. R. Sheeley, J. A. Davies, L. F. Burlaga, N. P. Savani, C. Jacquey, and R. J. Forsyth (2010c), White light and in situ comparison of a forming merged interaction region, *Astrophys. J.*, *719*, 1385–1392, doi:10.1088/0004-637X/719/2/1385.

Sheeley, N. R., Jr., H. Walters, Y.-M. Wang, and R. A. Howard (1999), Continuous tracking of coronal outflows: Two kinds of coronal mass ejections, *J. Geophys. Res.*, *104*, 24,739–24,767, doi:10.1029/1999JA900308.

Sheeley, N. R., et al. (2008), Heliospheric images of the solar wind at Earth, *Astrophys. J.*, *675*, 853–862, doi:10.1086/526422.

Smith, A., et al. (2012), Galaxy Zoo Supernovae, *Mon. Not. R. Astron. Soc.*, in press.

Stone, E. C., et al. (1998), The Advanced Composition Explorer, *Space Sci. Rev.*, *86*, 1–22, doi:10.1023/A:1005082526237.

Tappin, S. J., and T. A. Howard (2009), Direct observation of a corotating interaction region by three spacecraft, *Astrophys. J.*, *702*, 862–870, doi:10.1088/0004-637X/702/2/862.

Tyasto, M. I., O. A. Danilova, L. I. Dorman, V. M. Dvornikov, and V. E. Sdobnov (2008), On the possibility to check the magnetosphere's model by CR: The strong geomagnetic storm in November 2003, *Adv. Space Res.*, *42*, 1556–1563, doi:10.1016/j.asr.2007.06.057.

Wang, Y.-M., and N. R. Sheeley Jr. (1990), Solar wind speed and coronal flux-tube expansion, *Astrophys. J.*, *355*, 726–732.

Williams, A. O., J. A. Davies, S. E. Milan, A. P. Rouillard, C. J. Davis, C. H. Perry, and R. A. Harrison (2009), Deriving solar transient characteristics from single spacecraft STEREO/HI elongation variations: A theoretical assessment of the technique, *Ann. Geophys.*, *27*, 4359–4368, doi:10.5194/angeo-27-4359-2009.

Williams, A. O., N. J. T. Edberg, S. E. Milan, M. Lester, M. Fränz, and J. A. Davies (2011), Tracking corotating interaction regions from the Sun through to the orbit of Mars using ACE, MEX, VEX, and STEREO, *J. Geophys. Res.*, *116*, A08103, doi:10.1029/2010JA015719.

J. A. Davies and C. J. Davis, RAL Space, Rutherford Appleton Laboratory, Chilton OX11 0QX, UK. (chris.davis@stfc.ac.uk)

M. Lockwood and M. J. Owens, Department of Meteorology, University of Reading, Reading RG6 6BB, UK.